



Published in final edited form as:

*Invest Ophthalmol Vis Sci.* 2009 October ; 50(10): 4873–4880. doi:10.1167/iovs.08-3291.

## Stimulus-Evoked Intrinsic Optical Signals in the Retina: Pharmacologic Dissection Reveals Outer Retinal Origins

Jesse Schallek<sup>1</sup>, Randy Kardon<sup>2</sup>, Young Kwon<sup>2</sup>, Michael Abramoff<sup>2</sup>, Peter Soliz<sup>3</sup>, and Daniel Ts'o<sup>1</sup>

<sup>1</sup>Department of Neurosurgery, SUNY Upstate Medical University, Syracuse, New York

<sup>2</sup>Department of Ophthalmology and Visual Science, University of Iowa, Iowa City, Iowa

<sup>3</sup>Vision-Quest Biomedical, Albuquerque, New Mexico

### Abstract

**Purpose**—To elucidate the anatomic origins of stimulus-evoked intrinsic optical signals in the mammalian retina by using selective pharmacologic blockade of specific retinal layers.

**Methods**—Four adult cats were used to investigate the stimulus-evoked intrinsic signals. The retinas were visually stimulated with a liquid crystal display (LCD) integrated into a modified fundus camera. The evoked signals in the near infrared (NIR) were recorded with a digital camera to image the changes in the optical reflectance of the retinas. Variants of the electroretinogram (pattern ERG and long-pulse ERG) were also recorded as additional measures of retinal function. Specific retinal layers were inactivated via intravitreal injections of the voltage-gated sodium channel blocker, tetrodotoxin (TTX), the metabotropic glutamate receptor (mGluR6) agonist, 2-amino-4-phosphonobutyric acid (APB), and/or the ionotropic glutamate receptor antagonist *cis*-2,3 piperidinedicarboxylic acid (PDA). The stimulus-evoked intrinsic signals were imaged before and after drug injection.

**Results**—ERG recordings and tests of the consensual pupillary response confirmed the effectiveness of each drug. Yet despite the pharmacologic blockade of the inner retina (TTX) and postreceptor retinal circuitry (APB and PDA), the stimulus-evoked intrinsic signals remained essentially unaltered from preinjection conditions. Similarly, the time course of the signal did not appreciably shift in time or shape.

**Conclusions**—The findings demonstrate that stimulus-evoked intrinsic signals persist after injection of APB, PDA, and TTX, drugs that work to suppress inner and postreceptor retinal circuitry. The persistence of the intrinsic signals after administration of these drugs indicates that the dominant intrinsic signals are likely to arise from the outer retina.

Several groups have reported the existence of stimulus-evoked intrinsic signals in the retina of mammals (Ts'o DY, et al. *IOVS* 2003;44:ARVO E-Abstract 2709; Ts'o DY, et al. *IOVS* 2004;45:ARVO E-Abstract 3495; Ts'o DY, et al. *IOVS* 2005;46: ARVO E-Abstract 2258;

Corresponding author: Daniel Ts'o, Department of Neurosurgery, SUNY Upstate Medical University, 750 E. Adams Street, Syracuse NY 13210; tsod@upstate.edu.

Disclosure: J. Schallek, None; R. Kardon, P; Y. Kwon, P; M. Abramoff, None; P. Soliz, VisionQuest Biomedical (E); D. Ts'o, P

Ts'o DY, et al. *IOVS* 2006;47:ARVO E-Abstract 5899; Ts'o DY, et al. *IOVS* 2007;48:ARVO E-Abstract 1957; Ts'o DY, et al. *IOVS* 2008;49:ARVO E-Abstract 2006).<sup>1-6</sup> The in vivo signals described by these groups show near-infrared (NIR) reflectance signals in response to visual stimulation. Typically, the signals reported by these groups show a latency of less than 500 ms and a time constant on the order of seconds. These studies have implemented a similar acquisition paradigm that separates the stimulus wavelengths from the reflectance wavelengths, thus enabling the recording of reflectance changes in the near-infrared that are not confounded by reflectance from the visible stimulus. We have used a modified fundus camera to show that the intrinsic signals demonstrate high colocalization with the stimulated retina (Ts'o DY, et al. *IOVS* 2003;44:ARVO E-Abstract 2709).<sup>1</sup> There are several proposed biophysical origins of the retinal signals including hemodynamics,<sup>5</sup> oximetric origins,<sup>7</sup> and light scattering.<sup>8-10</sup> Although the relative contributions from each of these sources is not yet fully established, an additional question remains: what are the anatomic origins of the in vivo signals?

To date, a few studies have provided suggestive evidence regarding the anatomic origins of these signals in the retina.<sup>2,4</sup> Yet, definitive evidence has been missing regarding the laminar origins. In this study, we focused our efforts to identify the contributions from specific retinal layers using three pharmacologic agents. By examining the signal characteristics before and after drug application, we directly tested the contribution of distinct retinal layers in a series of experiments. In the first experiment, we made intravitreal injections of tetrodotoxin (TTX) to suppress the spiking activity of the innermost retinal layers consisting of ganglion cells, their axons, and spiking amacrine cells.<sup>11</sup> The action of TTX targets voltage-gated sodium channels and thus suppresses the spiking potential of the inner retina while leaving middle and outer retinal cell function intact.<sup>11-13</sup>

In a second experiment, we examined the contribution of other retinal layers by injecting drugs that act on the photoreceptor–bipolar cell junction. Intravitreal injections of 2-amino-4-phosphonobutyric acid (APB) blocked photoreceptor input to the ON bipolar cells of the retina,<sup>14</sup> whereas *cis*-2,3-piper-idinedicarboxylic acid (PDA) suppressed the response of OFF bipolar cells, horizontal cells, and other cells containing ionotropic glutamate receptors (iGluR) downstream of both ON and OFF pathways.<sup>15</sup> When injected together, these drugs suppress the stimulus-evoked potential at the level of the bipolar cell input, while leaving photoreceptor function intact.<sup>15</sup> Moreover, administering these drugs together not only attenuates bipolar cell response, but also suppresses the majority of postreceptor function in the retina.<sup>16</sup> We report that application of these drugs has minimal affect on the spatial attributes or strength of the intrinsic retinal signals, suggesting that these signals arise from outer retinal function.

## Methods

### Animals and Preparation

We imaged the retinas of four adult healthy cats between the ages of 1 and 2.4 years. Preparation is described in detail in the accompanying paper.<sup>6</sup> Briefly, the cats were anesthetized with sodium thiopental and paralyzed with vecuronium bromide for imaging stability. The pupils were dilated and accommodation was inhibited with neosynephrine and

atropine drops. Contact lenses were placed in the eyes to prevent the corneas from drying. The investigation adhered to the ARVO Statement for the Use of Animals in Ophthalmic and Vision Research. The cats were cared for in accordance with the Animal Welfare Act and the Department of Health and Human Service (DHHS) Guide for the Care and Use of Laboratory Animals.

### Stimuli and Imaging

Stimulus and imaging parameters are described in detail in the accompanying paper.<sup>6</sup> Briefly, we used patterned visual stimuli consisting of vertical and horizontal bars positioned on a Cartesian grid. Visual stimuli were band-pass filtered ( $540 \pm 30$  nm) to maximally stimulate the retina, while not infringing on the near infrared (NIR) interrogation wavelengths (the wavelengths at which reflectance measurements were made, 700–900 nm). Stimulus intensities were between 3 and 7.7 cd/m<sup>2</sup>, presented against a low-mesopic background of 0.12 cd/m<sup>2</sup> (background intensity of the LCD). The animals were adapted to the background level for 1 hour or more before imaging. A dim NIR light was continuously on and diffusely illuminated the fundus. The fundus reflectance was recorded with a charge-coupled device (CCD) camera. The camera collected a sequence of 20 frames collected at two Hz. The stimulus paradigm consisted of imaging 2 seconds of baseline reflectance (no stimulus), 3 seconds of stimulus, followed by 5 seconds of poststimulus reflectance.<sup>6</sup> NIR fundus images were examined in real time and also stored for more detailed analysis.

### Focal Electroretinogram

An eye speculum spanning the inferior and superior fornix was used as a transcorneal electrode. A speculum placed in the unstimulated eye served as a reference electrode, and a ground electrode was placed on the stereotaxic frame. ERG waveforms were band-pass filtered between 0.5 and 55 Hz and amplified 10,000×. Waveforms were then digitally acquired with a custom software program (MatLab; The Math-Works, Natick, MA) sampling at 400 Hz. Typically, 60 waveforms were averaged online before data were saved.

Stimuli were “long-duration focal ERGs” spanning 35° to 45°. Background light levels were on the order of  $1 \times 10^{-2}$  cd/m<sup>2</sup> with a 500-ms luminance step to 8 cd/m<sup>2</sup>. This method was favorable over Ganzfeld flash ERGs for two reasons. First, the focal ERGs were evoked with the same LCD device used to generate stimuli for the intrinsic signals. Second, a long-duration luminance step allowed us to temporally separate the ON and OFF response of the retina.

### Pattern Electroretinogram

The eye was stimulated with the LCD/modified fundus camera setup described earlier. The visual stimulus consisted of a counterflickering checkerboard pattern with a field size of approximately 40° field of view. Check sizes were between 0.4° to 3.2°. Temporal frequency was at a fixed rate of 12 reversals/s with a Michelson contrast value of 96.9%. We averaged 60 to 200 pattern (p)ERG waveforms before data were saved for later analysis.<sup>17</sup>

## Drug Preparation

All pharmacologic agents were dissolved in a bacteriostatic, balanced salt solution (BSS; Alcon, Fort Worth, TX), and filtered with a 0.2- $\mu\text{m}$  filter before each experiment. A total volume of 40 to 80  $\mu\text{L}$  was injected into either the right or the left eye. Final concentrations of 4.8 to 8.4  $\mu\text{M}$  tetrodotoxin (TTX), 0.83 to 3.8 mM 2-amino-4-phosphonobutyric acid (APB), and 3.3 to 3.8 mM *cis*-2,3-piperidinedicarboxylic acid (PDA) were based on a vitreous volume estimate of 2.1 mL.<sup>18</sup> These concentrations are within the range of significant suppression of the ganglion cells and the ON and OFF pathways.<sup>11</sup>

## Drug Injection

Before drug injection, the eye was treated with an ophthalmic anesthetic (0.5% proparacaine hydrochloride) to minimize discomfort. A 28- to 30-gauge needle was inserted posterior to the limbus and angled toward the center of the vitreous humor to ensure drug delivery and avoidance of the lens. After visual verification of needle placement, a slow controlled push of the syringe expelled the drug into the vitreous and the needle was held in place for 30 seconds before removing the needle. In the case of the APB+PDA injections, two separate injections were made within minutes of each other in the nasal–superior and temporal–superior angles.

## Image Analysis

Details of off-line analysis are described in detail in the accompanying paper.<sup>6</sup> Our analysis focused on quantifying the signal intensity and time course in user-defined regions of interest (ROIs). ROIs were positioned over areas demonstrating strongest and most consistent signal (Fig. 1A). Difference frame analysis was analyzed in a custom program (MatLab; The Mathworks). The data are reported as fractional change in reflectance ( $dR/R$ ).<sup>6</sup>

## Results

### Baseline Characteristics of Stimulus-Evoked Intrinsic Signals

Signal characteristics in noninjected eyes were consistent with a much larger data set (shown in the accompanying paper<sup>6</sup>). Briefly, intrinsic signals showed tight spatial correlation with the stimulated region of the retina. Focal activations matching the stimulus pattern showed a negative signal (decrease in reflectance) underlying the stimulus with an adjacent positive signal (increase in reflectance, Fig. 1A). Intrinsic signals could be evoked throughout many locations in the retina, although data reported here are typically 0° to 30° around the area centralis. The stimulus paradigm we used revealed characteristic temporal properties shown in Figure 1B. Both negative and positive signals were observed within 500 ms of stimulus onset and monophasically increased in intensity until the stimulus is turned off. Within several seconds of stimulus termination, the intensity of positive and negative signals waned back toward baseline reflectance values ( $dR/R = 0$ ). This imaging paradigm was maintained in all experiments to provide consistency for before and after drug treatment conditions.

## Effect of TTX on Intrinsic Signals

We used the above observations to characterize the normal conditions and compared the results to the TTX treated retina. Both intrinsic signal and ERG data were collected from three independent experiments on two cats. The normal, untreated response to a vertical bar is seen at the top of Figure 2A (black outline). Within an hour of these data, a single TTX injection was made into one eye of each cat. We imaged the retina again at least 1 hour after injection. The intrinsic signals after TTX are shown in the bottom row in Figure 2A (gray outline). The position, strength, and colocalization of the signals remain intact after the TTX injection. This finding was consistent across all three experiments.

We also examined the intrinsic signal magnitude and time course. Several regions of interest (ROIs) were positioned over the patterned response in preinjection conditions (example, Fig. 1). The same ROI positions were examined after the injection. The before- and after-TTX time course from two individual experiments can be seen in Figure 2B. As expected from previous experiments, the pre-TTX signal (black trace) showed typical baseline activity for 2 seconds, a signal development period while the stimuli was presented, and a recovery phase when the stimulus was turned off. After TTX injection (gray trace), the signal magnitude was nearly identical with the preinjection condition. Comparisons of the pre- and postinjection means show only a 6% decrease in signal at the maxima. This change is unremarkable when compared with the normal variability of the system described by 14.3% (1 SEM) at the same time points (Fig. 2C). In addition to a relatively unchanged magnitude, the major components of the time course remained the same. The post-TTX signals show the same rise- and recovery-phase dynamics as the preinjection condition. The results of these experiments show that TTX has minimal effect on the strength or time course of the predominant intrinsic signals.

As a control for the effectiveness of the TTX, we performed two additional tests of retinal function, the pERG and the consensual pupillary light reflex. In the pERG test, a 6-Hz counterflickering checkerboard stimulus induced a frequency-doubled response that matched the reversal rate of the patterned stimulus (Fig. 3, top row, black trace). After TTX, the amplitude of the pERG was attenuated (gray trace). The power spectrum of the pERG was calculated with a fast-Fourier transform (FFT; Fig. 3, middle row). The peak corresponding to contrast reversal component was attenuated between 40% to 99% after administration of TTX (on average, power decreased by two orders of magnitude). This change is consistent with the blockade of ganglion cell function (in primates).<sup>11</sup> In addition, all animals were tested for the absence of the consensual pupillary light reflex. In this test, a bright light presented to the drug-treated eye produced no consensual pupillary constriction in the untreated eye. This result is consistent with silenced ganglion cell function in the treated eye, as no signal reached the Edinger-Westphal nucleus to cause the bilateral constriction. Before the injection, each cat demonstrated a strong consensual pupillary light reflex, whereas after the injection, the consensual pupillary light reflex was undetectable. These controls, consistent in all three experiments, are evidence of the effectiveness of the TTX injection.

To test the ganglion cell contribution to the intrinsic functional signal using a completely different methodology, we examined the signal dependency on spatial contrast and spatial frequency. If indeed intrinsic signals arise from ganglion cell origins, we may expect to see

intrinsic signals display similar spatial frequency tuning functions.<sup>19,20</sup> To test this notion, the retinal response to a patterned set of four spatial frequencies between 0.4° and 3.2° check size were examined (Fig. 4, Cond. 1). The maximum amplitude of the signal is plotted in the dark bar histogram in Figure 4. The data show very little modulation in response to different spatial frequencies, inconsistent with the physiology of ganglion cells.<sup>20</sup> Luminance recordings were made with a spectrophotometer to make sure the time-averaged energy of each stimulus was the same.

To isolate a potential spatiotemporal contrast signal, we elevated the luminance of the background to be equivalent to the time-averaged energy of the stimulus. Simply stated, we set the stimulus background from black to gray, which matched the time-averaged luminance of the counterflickering black-and-white checks. In this case, the functional images driven by dynamic patterned stimuli did not reveal any detectable signal (Fig. 4). Of interest, when we quantified the reflectance change over the patterned-stimulus region of retina, the response was similar to the baseline noise in the blank condition. This finding was true for all spatial frequencies tested, yielding no spatial-frequency tuning function. Taken together, these findings are consistent with the TTX experiments, in which evidence showed that ganglion cells did not contribute to the predominant negative intrinsic signals.

### Effect of APB Injection on Signal Properties or Dynamics

To examine other retinal contributions, we selected APB to suppress ON bipolar cell function.<sup>14</sup> The silencing of the ON pathway was examined first, because intrinsic signals initiate within 500 ms of stimulus onset and continue to grow in strength as long as the stimulus stays on.<sup>6</sup> This finding is present with dynamic (counterflickering) as well as static (solid) stimuli. Similar to the findings with TTX, we did not find any robust effects of APB on the signal properties. Strong negative signal responses were observed both before and after APB injection. Figure 5A shows the retinal response of one cat to a vertical (left) and a horizontal (right) bar stimulus. After injection of APB, the signal remained spatially specific and strongly colocalized to the stimulated region of retina. This finding was consistent across all stimulus conditions tested. We quantified the result by positioning ROIs over regions showing the strongest signal before injection and then re-examined at least 1 hour after injection (Fig. 5C). The signal mean after APB was 6.1% lower than the normal condition (averaged between 2.5 and 10 seconds: the stimulus and poststimulus epochs). This value is relatively small considering the SEM for the non-injected condition was 13.3% for the same time epoch. At the signal maxima (measured at 5.5 seconds) APB data showed a signal reduction of 16.6% compared with normal. This value is also small considering the noise of the normal system is represented by  $\pm 18.2\%$  SEM at the same maxima. Moreover, when we examined the time course of the signal, we observed a similar onset, rise time, rise slope, and recovery phase of the signal. In short, APB failed to substantially change the signal characteristics, which indicates that ON channel components were not the origin of the predominant intrinsic signals.

Our control ERGs for drug action were consistent with the specific pharmacology of APB. APB has a very specific effect on the depolarizing bipolar cells of the retina.<sup>14</sup> In this case, we used a long-pulse (step-wise) ERG instead of the pERG or Ganzfeld flash ERG, because



it allows separation of the ON and OFF components. Figure 5B shows the long-pulse ERG of the same cat before and 1 hour after APB injection. The b-wave was strongly reduced in these experiments, but not completely eliminated (Fig. 5B, arrow), whereas the d-wave potential, which originates from the OFF channel remained largely intact (Fig. 5B, arrowhead). The ERG result is consistent with the specificity of APB to suppress the ON channel activity in the retina.

### **Persistence of Intrinsic Signals after APB+PDA Intravitreal Injections**

Results from the previous two sets of experiments revealed that the predominant signals did not arise from the ganglion cell layer (evidence from TTX) or the ON channel components (APB evidence). With these data considered, we turned to the use of a cocktail of APB +PDA, to suppress both the ON and OFF channels in the retina. The pharmacology of PDA acts to suppress the input to OFF bipolar cells and horizontal cells, while leaving photoreceptor function intact.<sup>15</sup> Together with the suppression of ON channel bipolar cells and their downstream components, we tested the contributions of the dominant populations of bipolar, horizontal, amacrine, and ganglion cell function on the intrinsic signals. The result after the dual injection of APB and PDA showed little change from the baseline condition. Figure 6A shows several stimuli conditions before and after the cocktail injection. The spatially specific signals in the control condition (black outline) remained highly colocalized after injection of the cocktail (gray outline). This result was consistent in two cats tested.

Similar to the results of the TTX and the APB-only injections, intrinsic signals showed negligible change in intensity. Magnitudes of the postinjection condition are within 10.2% of the preinjection condition at the signal maxima. This value is well within 1 SEM, ranging between 12% and 18% for the post- and precocktail analyses, respectively. In addition, the ROI analysis revealed that the time course remains consistent (Fig. 6C), with no notable advance or lag of either the rising or falling components of the signal.

As a control, we recorded the long-duration ERG in conjunction with intrinsic signal recordings. Figure 5B shows the injected drugs had the desired effect. APB suppression of the b-wave (ON component), as well as a reduction in d-wave (OFF-component) revealed a negative response that was most likely the preserved photoreceptors' contribution to the ERG. The attenuated ON and OFF response was observed after the cocktail was injected in both cats. Consistent with this finding, both cats showed no consensual pupillary response 1 hour after drug application, indicating a successful blockade of post-receptoral evoked potentials to downstream cell types (Fig. 7).

These findings from the APB and PDA cocktail experiments corroborated data from the TTX and APB experiments: that ganglion cells and ON channel cells were not the origins of the predominant intrinsic signals. Moreover, the APB+PDA experiment revealed that the postreceptoral OFF channel components also were not the origin of the intrinsic signal.

## Discussion

This study was conducted to elucidate the origins of intrinsic signals in the retina. Pharmacologic suppression of the ganglion cell layer with TTX as well as postreceptoral cell types with APB+PDA showed negligible effects on the magnitude, time course or spatial specificity of the intrinsic signals. This finding suggests that the dominant spatial intrinsic signals do not originate in the inner retina.

### Laminar Origins of the Signal

We chose specific pharmacologic agents to selectively suppress different components of the retinal circuit. In the TTX experiments, the pERG response was strongly attenuated after injection, consistent with the pharmacology of suppressed inner layers,<sup>11</sup> yet intrinsic signals remained essentially unchanged. This finding leads to the conclusion that ganglion cells and spiking amacrine cells contribute minimally to the intrinsic signals that we have reported. The result corroborated with those of additional experiments that showed that intrinsic signals do exhibit show spatial-frequency tuning (Fig. 4). Rather than being responsive to stimulus contrast, signals were found to correlate with absolute stimulus luminance. Since ganglion cells have a characteristic spatial-frequency tuning and respond best to stimulus contrast,<sup>19,20</sup> our findings are inconsistent with the idea that the signals arise primarily from ganglion cells. Although our data do not support ganglion cell contribution to the dominant signals, it is possible that ganglion cells do contribute to other intrinsic signals beyond those we are reporting.

Our findings support a different conclusion than two recent reports in which the investigators also used TTX to explore retinal intrinsic signal origins (Okawa Y, et al. *IOVS* 2007;48: ARVO E-Abstract 3845).<sup>21</sup> These researchers found that TTX can suppress certain components of the intrinsic signal. In the study of Okawa et al., the optic nerve was stimulated to produce retrograde stimulation of retinal ganglion cells to generate intrinsic signals. Our findings did not rule out that ganglion cells can produce intrinsic signals when stimulated by high, nonphysiological levels. We activated the ganglion cells considerably less than the retrograde stimulation used by Okawa et al. Under our visual stimulus conditions, a ganglion cell signal may be masked by the dominant signals that we report.

Hanazono et al.<sup>21</sup> imaged the intrinsic signals in the primate retina 1 day after a TTX injection. Unlike our post-TTX results, they found that the extrafoveal signals showed a response decrease. Several differences may account for the discrepancy with our findings. First, the different results may be due to a species difference between the cat and monkey retina. Second, our mesopic, patterned stimuli produced spatially specific activations that are markedly different from the global flash-evoked responses used by Hanazono et al. A high-intensity flash stimulus may reveal a ganglion cell signal that we have not yet observed. Perhaps most notably, the discrepancy may be due to differences in elapsed time after TTX injection before the signals were recorded. In contrast to our 1-hour wait time, Hanazono et al. imaged the retina 1 day after TTX injection. This longer interval may have invoked secondary effects that reduced the optical signal, such as an increased intraocular pressure, optical complications, and other undesired effects induced by the invasive injection procedure and prolonged ganglion cell suppression. We specifically attempted to avoid such



complications by recording shortly after TTX was demonstrated to be effective. We observed a complete suppression of ganglion cell activity within 1 hour of the TTX injection, as confirmed by the absence of a consensual pupillary reflex and a strongly attenuated flicker frequency component in the pERG.

Blockade of signal transmission from photoreceptors to ON and OFF pathways using APB +PDA did not appreciably change the properties of the retinal intrinsic signals. We confirmed the blockade by recording long-pulse ERGs that showed the attenuation (though not elimination) of the b- and d-wave components.<sup>11,14–16,22</sup> Our imaging results using APB and PDA make it unlikely that inner retinal components contribute to a strong metabolic<sup>23</sup> or light-scattering signal.<sup>9</sup> In sum, our experiments using pharmacologic agents allow us to conclude that bipolar cells, horizontal cells, amacrine cells, and ganglion cells are not the origin of the dominant intrinsic signals. Instead our findings indicate an outer retinal origin of the stimulus-evoked signals.

Other studies also support the presence of functional optical signals from the outer retina, particularly the photoreceptors.<sup>4,8,24</sup> NIR signals reported by Pepperberg et al.<sup>8</sup> showed a fast response with a time to peak on the order of milliseconds, much faster than our rise time, on the order of seconds. It is worth noting that Pepperberg et al. performed the signals in an in vitro, blood-free preparation.

The signals we report may be metabolic, as are the signals in the neocortex. The wavelength-dependent spectra of the signals in the accompanying paper<sup>6</sup> provides evidence consistent with a metabolism-driven signal in the retina. A possible signal source may be from hemodynamic changes caused by stimulated photoreceptors. This hypothesis is plausible due to the large differences in metabolic consumption from activation of rods and cones.<sup>25–27</sup> In the neocortex, stimulus-evoked blood flow changes<sup>23,28</sup> or oximetry (oxygen delivery),<sup>23,29</sup> strongly contribute to cortical signals. Thus, in the retina, it is also possible that the photoreceptor activity can locally modulate hemodynamics. We should emphasize that we presently do not have data that directly show this relationship; rather, given our findings with TTX, APB, and PDA, it is the next logical avenue of exploration.

From our results, we conclude that the dominant signals are not dependent on the spiking activity in the inner retina (ganglion cells) as evidenced by persistence after TTX injection. Intrinsic signals do not demonstrate spatial frequency tuning, a known property of retinal ganglion cells. Signals remain after pharmacologic blockade of postreceptor function using APB and PDA. Given these findings, the signals we observe are likely to originate from the outer retinal layers (e.g., photoreceptors, retinal pigmented epithelium, and choroid).

## Acknowledgments

The authors would like to thank Mark Zarella, Dorothy Joiner, and Sandra McGillis for help with data collection and helpful discussions.

Supported by the National Institutes of Health NIBIB (National Institute of Biomedical Imaging and Bioengineering) Grant EB002843 and the Glaucoma Research Foundation.

## References

1. Abramoff MD, Kwon YH, Ts'o D, et al. Visual stimulus-induced changes in human near-infrared fundus reflectance. *Invest Ophthalmol Vis Sci.* 2006; 47:715–721. [PubMed: 16431972]
2. Tsunoda K, Oguchi Y, Hanazono G, Tanifuji M. Mapping cone- and rod-induced retinal responsiveness in macaque retina by optical imaging. *Invest Ophthalmol Vis Sci.* 2004; 45:3820–3826. [PubMed: 15452094]
3. Hanazono G, Tsunoda K, Shinoda K, Tsubota K, Miyake Y, Tanifuji M. Intrinsic signal imaging in macaque retina reveals different types of flash-induced light reflectance changes of different origins. *Invest Ophthalmol Vis Sci.* 2007; 48:2903–2912. [PubMed: 17525227]
4. Grieve K, Roorda A. Intrinsic signals from human cone photoreceptors. *Invest Ophthalmol Vis Sci.* 2008; 49:713–719. [PubMed: 18235019]
5. Nelson DA, Krupsky S, Pollack A, et al. Special report: noninvasive multi-parameter functional optical imaging of the eye. *Ophthalmic Surg Lasers Imag.* 2005; 36:57–66.
6. Schallick J, Li H, Kardon R, et al. Stimulus-evoked intrinsic optical signals in the retina: spatial and temporal characteristics. *Invest Ophthalmol Vis Sci.* 2009; 50:4865–4872. [PubMed: 19420337]
7. Hickam JB, Frayser R, Ross JC. A study of retinal venous blood oxygen saturation in human subjects by photographic means. *Circulation.* 1963; 27:375–385. [PubMed: 13961118]
8. Pepperberg DR, Kahlert M, Krause A, Hofmann KP. Photic modulation of a highly sensitive, near-infrared light-scattering signal recorded from intact retinal photoreceptors. *Proc Natl Acad Sci U S A.* 1988; 85:5531–5535. [PubMed: 3399504]
9. Cohen LB. Changes in neuron structure during action potential propagation and synaptic transmission. *Physiol Rev.* 1973; 53:373–418. [PubMed: 4349816]
10. Yao XC, George JS. Dynamic neuroimaging of retinal light responses using fast intrinsic optical signals. *Neuroimage.* 2006; 33:898–906. [PubMed: 17000120]
11. Hare WA, Ton H. Effects of APB, PDA, and TTX on ERG responses recorded using both multifocal and conventional methods in monkey. *Doc Ophthalmol.* 2002; 105:189–222. [PubMed: 12462444]
12. Viswanathan S, Frishman LJ, Robson JG, Harwerth RS, Smith EL 3rd. The photopic negative response of the macaque electroretinogram: reduction by experimental glaucoma. *Invest Ophthalmol Vis Sci.* 1999; 40:1124–1136. [PubMed: 10235545]
13. Hood DC, Frishman LJ, Viswanathan S, Robson JG, Ahmed J. Evidence for a ganglion cell contribution to the primate electroretinogram (ERG): effects of TTX on the multifocal ERG in the macaque. *Vis Neurosci.* 1999; 16:411–416. [PubMed: 10349962]
14. Slaughter MM, Miller RF. 2-Amino-4-phosphonobutyric acid: a new pharmacological tool for retina research. *Science.* 1981; 211:182–185. [PubMed: 6255566]
15. Slaughter M, Miller R. An excitatory amino acid antagonist blocks cone input to sign-conserving second-order retinal neurons. *Science.* 1983; 219:1230–1232. [PubMed: 6131536]
16. Bush R, Sieving P. A proximal retinal component in the primate photopic ERG a-wave. *Invest Ophthalmol Vis Sci.* 1994; 35:635–645. [PubMed: 8113014]
17. Bach M, Hawlina M, Holder GE, et al. Standard for pattern electroretinography: International Society for Clinical Electrophysiology of Vision. *Doc Ophthalmol.* 2000; 101:11–18. [PubMed: 11128964]
18. Frishman LJ, Steinberg RH. Intraretinal analysis of the threshold dark-adapted ERG of cat retina. *J Neurophysiol.* 1989; 61:1221–1232. [PubMed: 2746322]
19. Ohzawa I, Freeman RD. Pattern evoked potentials from the cat's retina. *J Neurophysiol.* 1985; 54:691–700. [PubMed: 4045545]
20. Enroth-Cugell C, Robson JG. Functional characteristics and diversity of cat retinal ganglion cells: basic characteristics and quantitative description. *Invest Ophthalmol Vis Sci.* 1984; 25:250–267. [PubMed: 6698746]
21. Hanazono G, Tsunoda K, Kazato Y, Tsubota K, Tanifuji M. Evaluating neural activity of retinal ganglion cells by flash-evoked intrinsic signal imaging in macaque retina. *Invest Ophthalmol Vis Sci.* 2008; 49:4655–4663. [PubMed: 18539934]

22. Evers HU, Gouras P. Three cone mechanisms in the primate electroretinogram: two with, one without off-center bipolar responses. *Vision Res.* 1986; 26:245–254. [PubMed: 3716218]
23. Frostig RD, Lieke EE, Ts'o DY, Grinvald A. Cortical functional architecture and local coupling between neuronal activity and the microcirculation revealed by in vivo high-resolution optical imaging of intrinsic signals. *Proc Natl Acad Sci U S A.* 1990; 87:6082–6086. [PubMed: 2117272]
24. Harary HH, Brown JE, Pinto LH. Rapid light-induced changes in near infrared transmission of rods in *Bufo marinus*. *Science.* 1978; 202:1083–1085. [PubMed: 102035]
25. Yu DY, Cringle SJ. Oxygen distribution and consumption within the retina in vascularised and avascular retinas and in animal models of retinal disease. *Prog Retin Eye Res.* 2001; 20:175–208. [PubMed: 11173251]
26. Stefansson E, Wolbarsht ML, Landers MB 3rd. In vivo O<sub>2</sub> consumption in rhesus monkeys in light and dark. *Exp Eye Res.* 1983; 37:251–256. [PubMed: 6628573]
27. Linsenmeier RA. Effects of light and darkness on oxygen distribution and consumption in the cat retina. *J Gen Physiol.* 1986; 88:521–542. [PubMed: 3783124]
28. Fukuda M, Rajagopalan UM, Homma R, Matsumoto M, Nishizaki M, Tanifuji M. Localization of activity-dependent changes in blood volume to submillimeter-scale functional domains in cat visual cortex. *Cerebral Cortex.* 2005; 15:823–833. [PubMed: 15459078]
29. Malonek D, Grinvald A. Interactions between electrical activity and cortical microcirculation revealed by imaging spectroscopy: implications for functional brain mapping. *Science.* 1996; 272:551–554. [PubMed: 8614805]

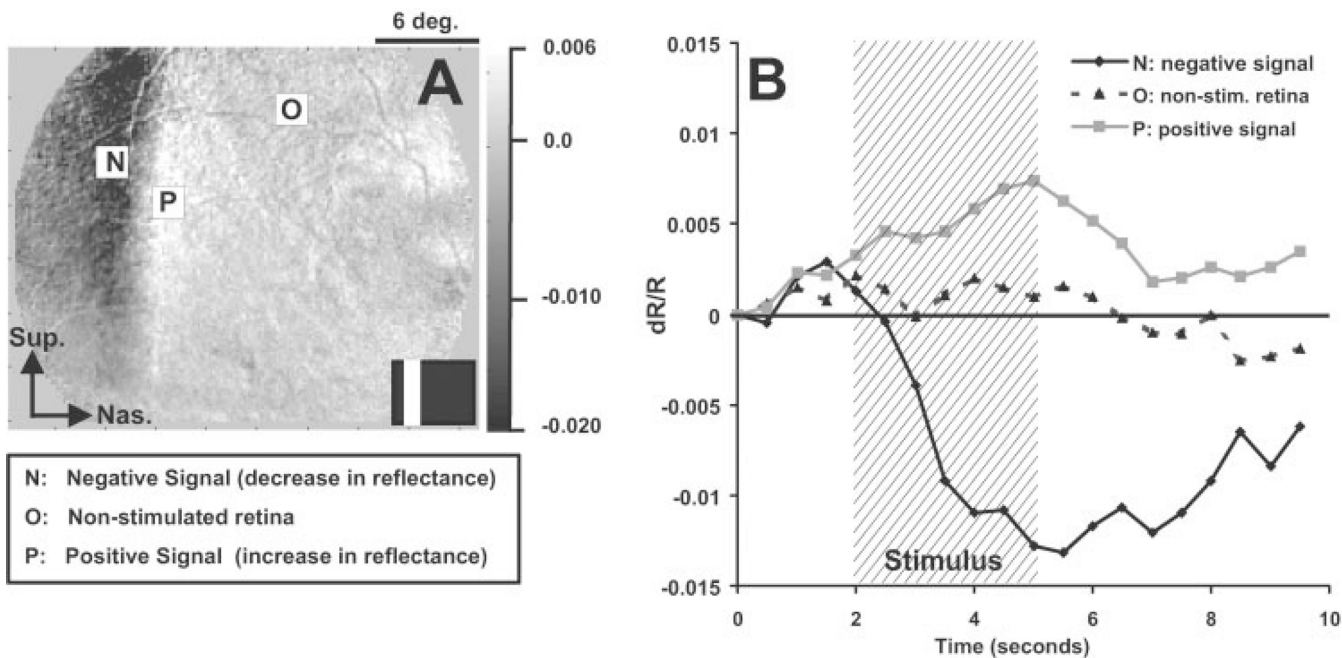


**Figure 1.**

Spatial properties and quantification method. **(A)** NIR response to a vertical bar on a dark background. The presentation of patterned visual stimuli produced two predominant signals of opposite polarity, a negative signal (N) and a positive signal (P), that were spatially adjacent. *Right:* Grayscale bar representing fractional change in reflectance ( $dR/R$ ). Negative signals correspond to a decrease in reflectance (*dark regions*). Conversely, positive signals correspond to a relative increase in reflectance (*light regions*). Areas that show no or slight reflectance change are *gray regions* ( $dR/R = 0$ ). The response is localized with the stimulated retina. Scale bar:  $6^\circ$  of visual angle. *Arrows:* superior and nasal directions in the fundus image. *Inset:* the stimulus used to evoke the response. **(B)** Fractional reflectance time course of three ROIs. The signal intensity is plotted as a function of time. The fractional reflectance for each ROI was calculated (see Schallek et al.<sup>6</sup>). Both the positive (ROI P, *white*) and negative signal (ROI N, *black*) showed negligible deviation from baseline during the prestimulus epoch (0–2 seconds). Between 2 and 5 seconds (stimulus on), both signals appeared and developed in magnitude. In the poststimulus epoch (5–10 seconds) both signals slowly recovered toward the baseline reflectance ( $dR/R = 0$ ). An ROI over the nonstimulated region of retina is also plotted (O, *dashed lines*). Reflectance changes were very small, most likely attributable to the biological noise of the system.

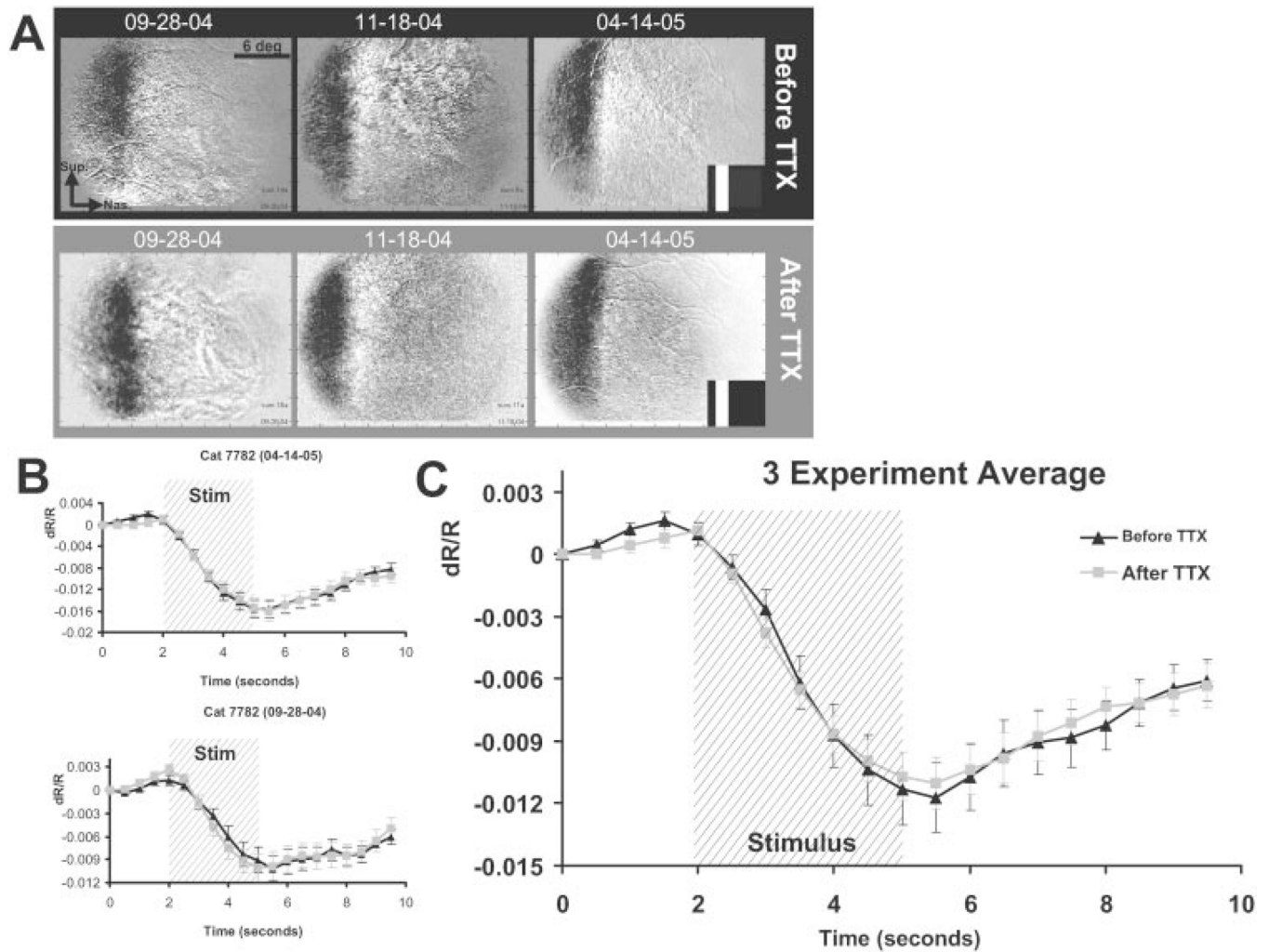


**Figure 2.**

Signal characteristics after TTX injection. (A) Signals persist after injection of TTX. Shown is the retina's response to a vertical bar stimulus before and after an injection of TTX from three separate experiments performed on different days. Signals remain strong and spatially specific after injection of TTX. (B) Negative signal time course from two independent experiments show the same characteristic shape and magnitude before (*black trace*) and after TTX injection (*gray trace*). (C) Data averaged from three experiments on two cats shows that the time course and magnitude of the signal is nearly indistinguishable. Error bars,  $\pm 1$  SEM. Before TTX, 30 ROI samples in three independent experiments. After TTX, 44 ROI samples in the same independent experiments.

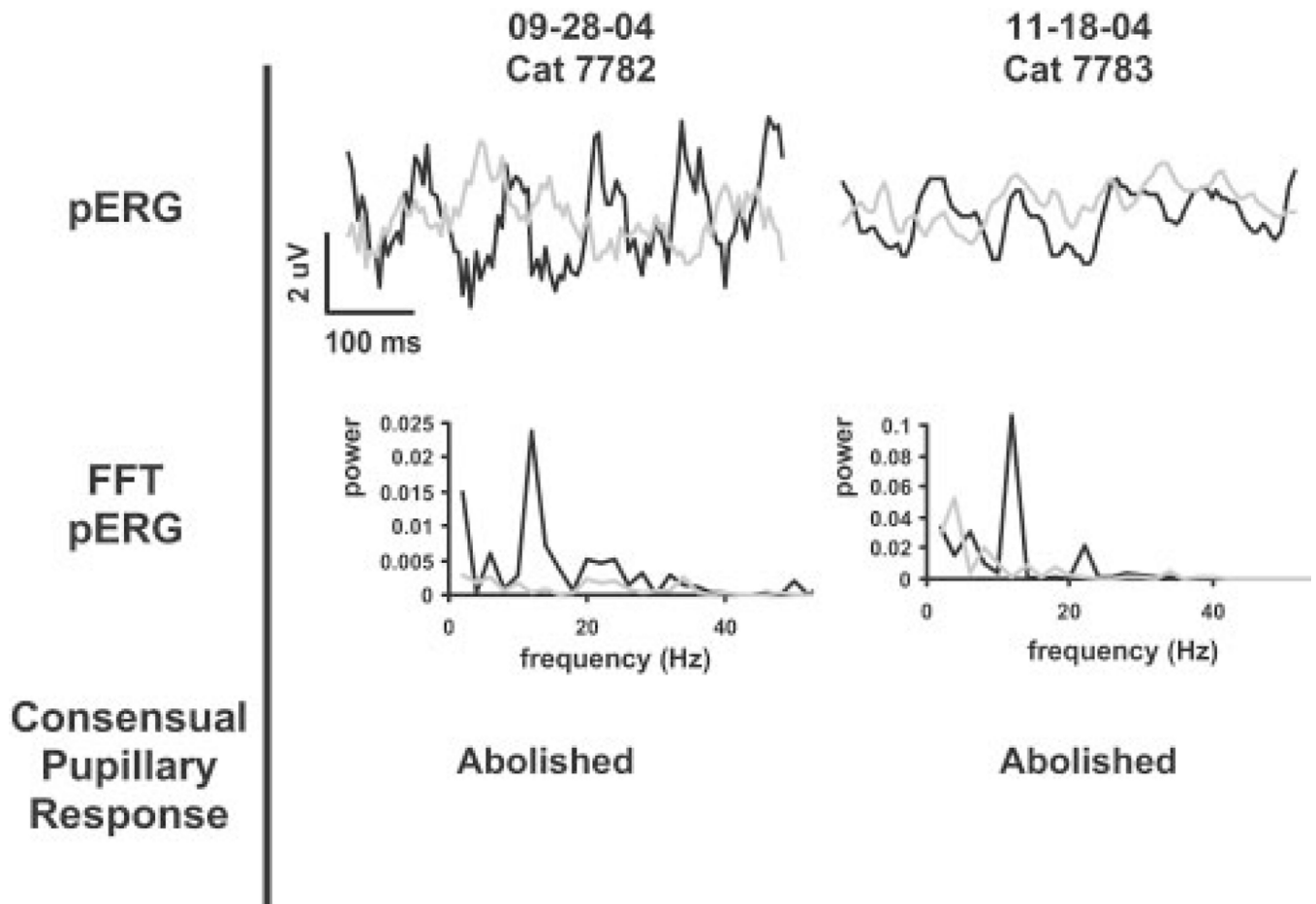


**Figure 3.**

Alternative measures of retinal function. Pattern ERG (pERG) responses were recorded in conjunction with optical imaging. *Top:* the pERG response from two animals injected with TTX. *Black trace:* the pERG response before injection, with a clear stimulus frequency-doubled response. At least 1 hour after injection (*gray trace*), the pERG showed minimal response corresponding to the reversal rate of the stimulus. *Middle:* the FFT power spectra of the raw pERG response. A strong 12-Hz component corresponding to the frequency-doubled response was seen in the noninjected condition, whereas after injection, the power at that frequency was attenuated by up to two orders of magnitude. *Bottom:* absence of the consensual pupillary reflex after injection (Abolished). The reflex was present before injection, but was abolished after injection indicating signal disruption to higher visual areas. Taken together, these findings confirm the desired suppression of ganglion cell function.



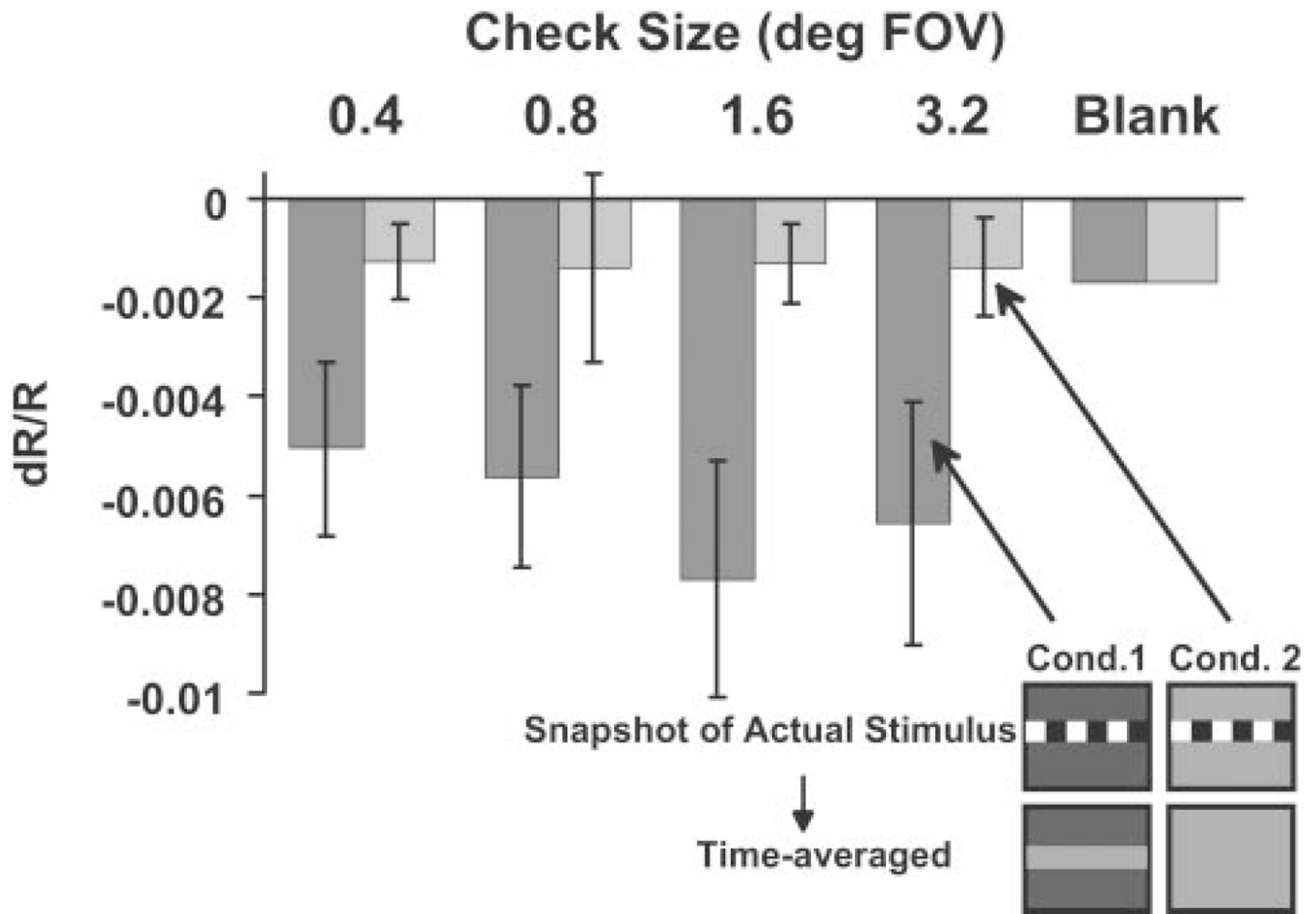


**Figure 4.** Signal dependence on spatial frequency components of the stimulus. Four different spatial frequencies (check size, between 0.4° and 3.2°) were randomly presented to the subject under two conditions. Condition 1 yielded a net stimulus increment against a dark background when time-averaged (*inset left*). This condition is represented by *dark bars* and shows minimal dependence on spatial frequency size. The second condition (*inset right*), was driven by presenting the same four test frequencies against a background that had the same time-averaged luminance as the stimulus (background light levels were equal to the integrated energy of the dark and light checks of the stimulus). In this condition (*light gray bars*), no signal was observed. ROIs positioned over regions where signals were once strong in the first condition yielded no detectable signal above noise levels (Blank). There was no tuning observed in this condition.

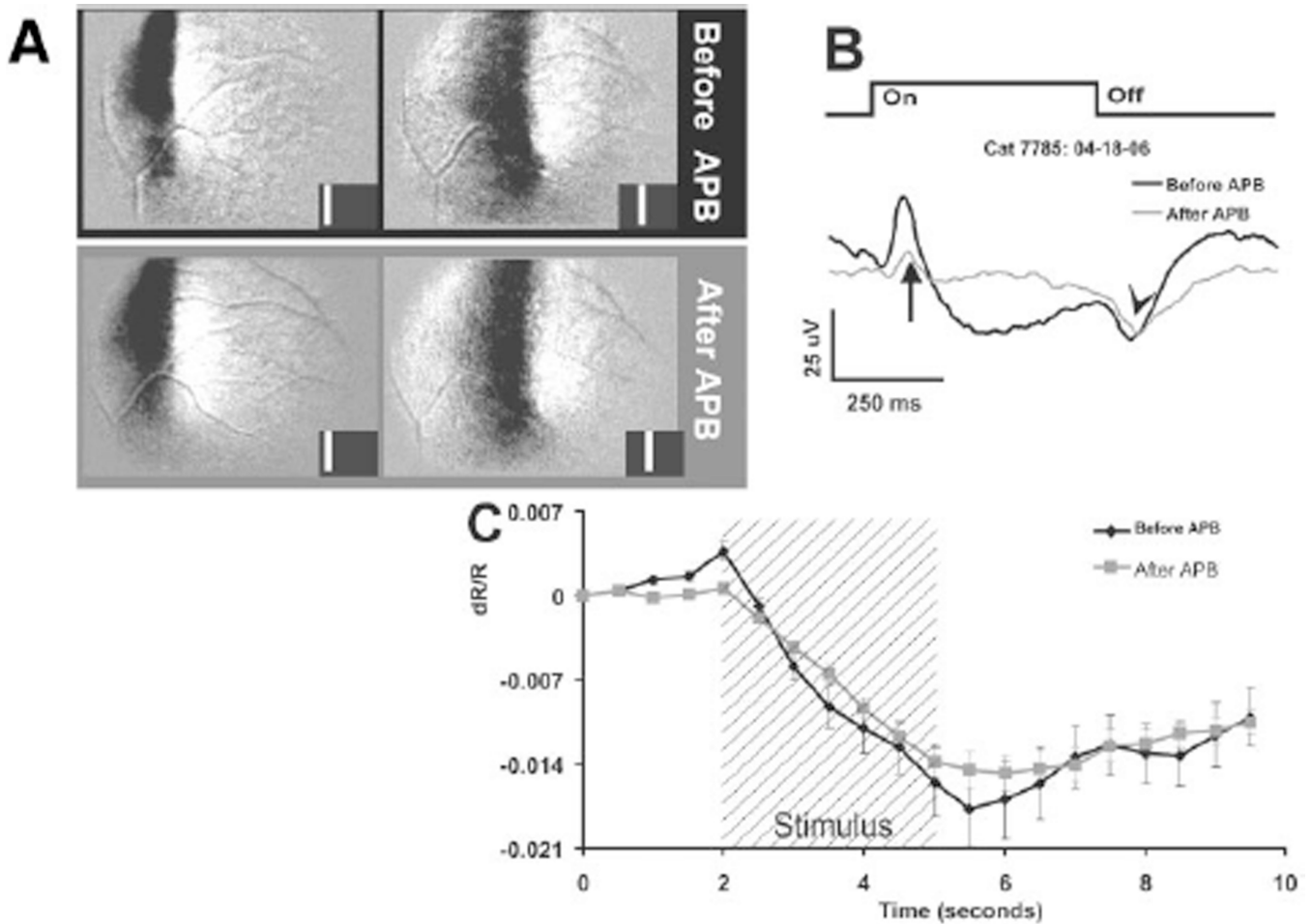


**Figure 5.**

Intrinsic signal properties after APB injection. (A) NIR response to two vertical stimuli. *Top*: the retinal response before injection; *bottom*: the response after injection of APB. Signals remained spatially specific and appeared relatively unchanged. (B) Long-pulse ERG before and after APB injection. A 0.5-second luminous pulse evoked a separate ON (*arrow*) and OFF response (*arrowhead*) in the normal condition (*black trace*). As expected, the ON component was strongly attenuated, whereas the OFF component remained strong 1 hour after APB (*gray trace*). (C) Signal time course before and after injection of APB. Several ROIs were examined before and reexamined after injection of APB. Before injection (*black trace*), a characteristic prestimulus baseline, stimulus-growth phase, and poststimulus recovery was observed. At least 1 hour after injection of APB, signals showed the same temporal characteristics. Signal magnitude remained largely the same. Preinjection, 18 measurements in one cat. Postinjection, 18 measurements in the same cat. Error bars,  $\pm 1$  SEM.

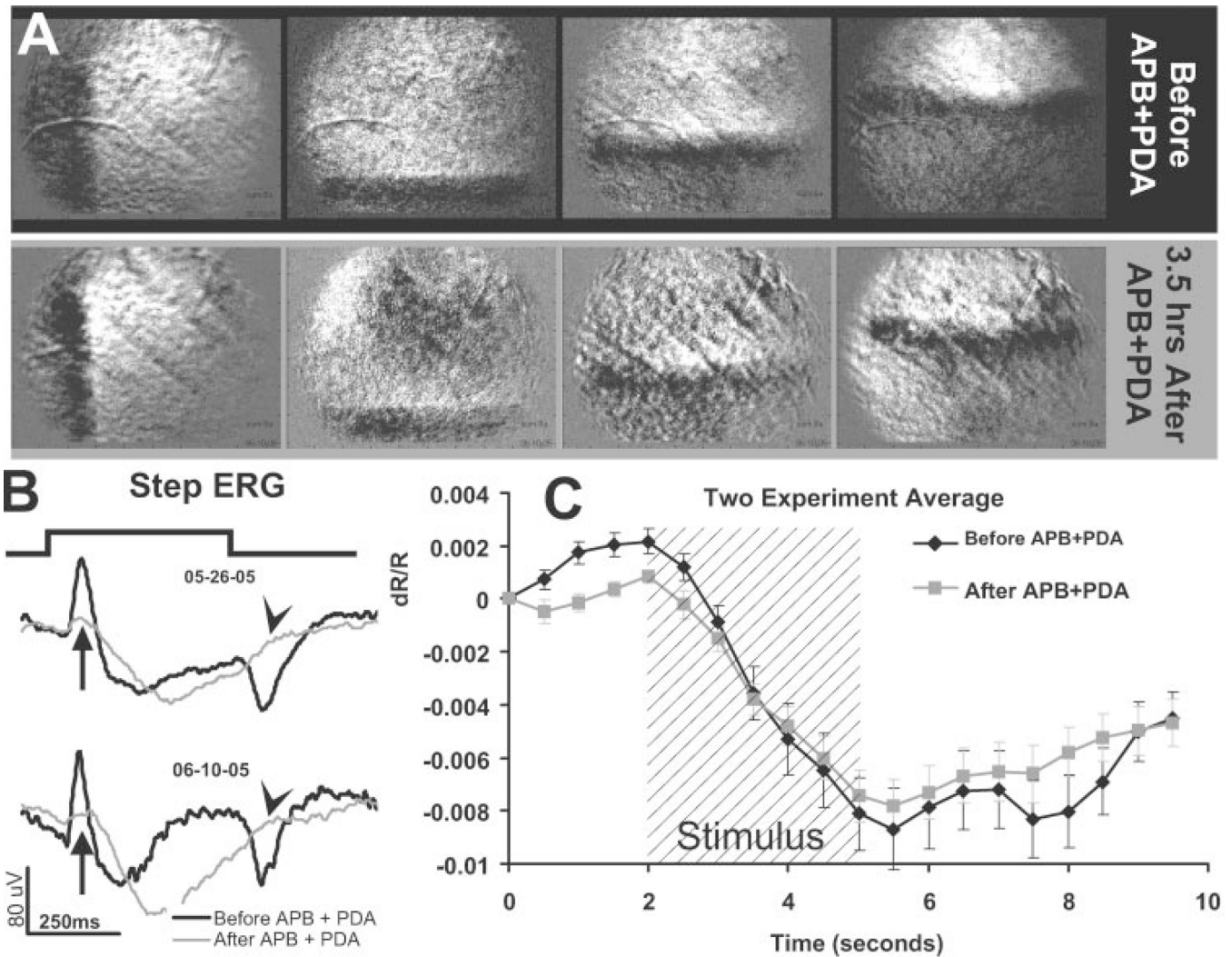


**Figure 6.**

Signals persist after APB+PDA injection. **(A)** The retina's response to several horizontal and vertical bars. *Top*: signals from the preinjected retina. *Bottom*: signals persist after combined injection of APB and PDA. **(B)** Long-pulse ERG before and after APB+PDA showed that both the ON (*arrow*) and OFF component (*arrowhead*) of the ERG were strongly attenuated after injection (*gray trace*) in each cat tested. **(C)** The averaged intrinsic signal time course from experiments performed on two cats. After intravitreal injection of APB+PDA (*gray trace*), signals showed the same characteristic baseline, stimulus, and recovery phases as in the normal condition (*black trace*). The magnitude after injection is within 10.2% of preinjection values. Preinjection, 27 measurements in two cats; postinjection, 62 measurements in the same two cats. Error bars,  $\pm 1$  SEM.

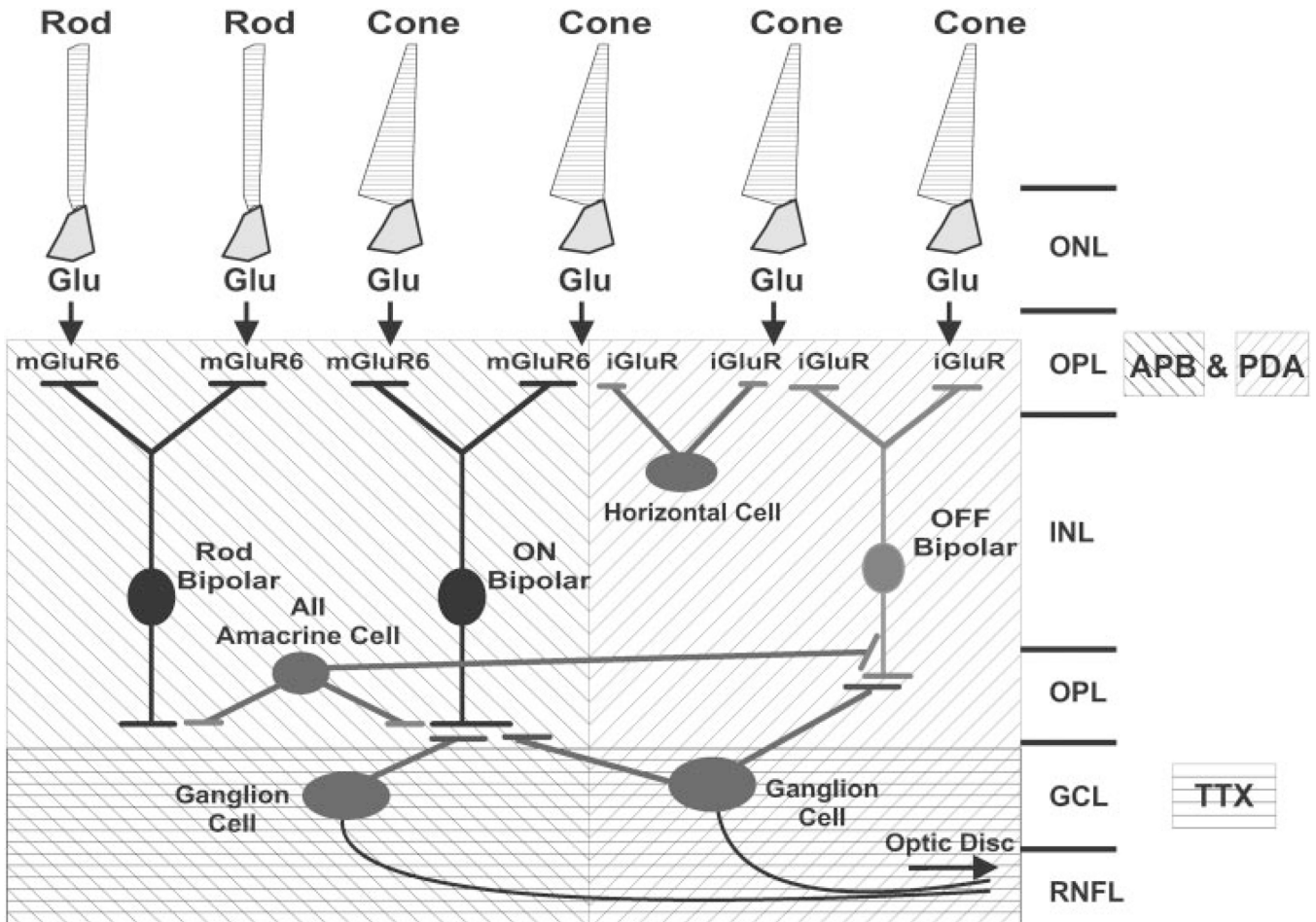


**Figure 7.**

A schematic of the drug action on specific retinal cell types. APB acts as an agonist for metabotropic glutamate receptors (mGluR6). APB not only disrupts postsynaptic ON bipolar cells, but as a consequence, attenuates cell function downstream in this pathway (ON pathway suppression, *left diagonal lines*). PDA acts on ionotropic glutamate receptors (iGluR) as an antagonist. PDA suppresses the efficacy of the photoreceptor-OFF bipolar cell junction. Likewise, cells downstream from this junction are functionally suppressed (*right diagonal lines*). TTX blocks voltage-gated sodium channels that are found primarily in the spiking cells of the retina. Its action is limited to the ganglion cells and a few types of spiking amacrine cells (suppression by TTX, *horizontally shaded region*). Glu, Glutamate; mGluR6, metabotropic glutamate receptor 6; iGluR, ionotropic glutamate receptor; ONL, outer nuclear layer; OPL, outer plexiform layer; INL, inner nuclear layer; GCL, ganglion cell layer; RNFL, retinal nerve fiber layer.